VERSITA

Cent. Eur. J. Chem. • 8(4) • 2010 • 766–782
DOI: 10.2478/s11532-010-0051-x

Central European Journal of **Chemistry**

Protolytic properties of the structurally rigid analogs of 2,6-distyrylpyridine. Widening the pH sensitivity range by the photochemical E→Z isomerisation and introduction of substituents capable to protolytic interactions

Research Article

Oleksiy V. Grygorovych[1], Oleksiy V. Nevskii[1], Sofia M. Moskalenko[1], Vasyl G. Pivovarenko[2], Andrey O. Doroshenko[1,*]

[1] *Institute for Chemistry at Kharkov V.N. Karazin National University, Kharkov 61077, Ukraine*

[2] *Department of Chemistry, Taras Shevchenko National University of Kyiv, Kyiv 01033, Ukraine*

Received 17 September 2009; Accepted 8 January 2010

Abstract: Protolytic interactions in the series of prospective fluorescent ratiometric wide-range pH indicators - structurally rigid analogs of 2,6-distyrylpyridine - (3E,5E)-3,5-dibenzylidene-8-phenyl-1,2,3,5,6,7-hexahydrodicyclopentano[b,e]pyridine - were investigated. The pyridine nitrogen atom basicity in these compounds is significantly lower in comparison with that of unsubstituted heterocycle and 2,6-distyrylpyridine. The photochemical E→Z photoisomerization and the side benzene rings substituents influence on the acid-base equilibria were studied. The complex multi-stage mechanism of the acid-base interactions of the polysubstituted compounds was elucidated. The most significant spectral effects were typical to the N,N-dialkylamino substituted compounds of the investigated series. The widest pH sensitivity interval covering nearly the full range of 0-14 units was demonstrated for compounds with both proton donor and proton acceptor substituents.

Keywords: *Dicyclopentano[b,e]pyridines • Electronic absorption spectra • Fluorescence spectra • Protolytic interactions • Wide range pH indicators • Photochemical E→Z isomerization.*

© Versita Sp. z o.o.

1. Introduction

During the last decades, biologically and medically oriented analysis was directed towards the miniaturization of both the studied objects and the sensing instruments. Fluorescence spectroscopy was often applied in line with such tendency because of its high sensitivity and ability to obtain analytical signal from the very low analytical volume.

A great number of multi-purpose fluorescent compounds have been developed [1]. Among these compounds, the pH and metal cations sensitive compounds are of particular interest because of their high potential for the practical application in the biological and medical analysis. Several classes of organic compounds are suitable for this purpose, for example cyanines [2,3] phthalocyanines [4,5], anthracenes [6], azlactone dyes [7], Shiff bases [8], and several other compounds [9]. The most interesting for the biophysical applications are the dyes with pH induced color changes in the "physiological" near-neutral range. For this purpose, Wolfbeiss and coworkers proposed several coumarin derivatives and 8-hydroxypyrenesulfonate [10,11]. Other investigators have also demonstrated similar applicability of fluorescein [12] and eosin – phenol red mixtures[13].

Several other groups focused their attention on the wide range pH indicators [14,15]. Such compounds can

* *E-mail: andrey.o.doroshenko@univer.kharkov.ua*

find practical application in the design of microsensors and fluorescent test systems [16]. Protolytic interactions were the background for the design of molecular switches, which analytical signal is the appearance/disappearance of fluorescence [17,18] or changing in the spectral composition of the emitted light [19].

Most of the known fluorescent dyes are of heterocyclic origin: xanthenes, coumarins, oxazoles, acridines, *etc.* [20], all of them are polycyclic condensed molecules with large conjugated π-system. The pyridine unit as a proton receptor part of the pH indicator was applied in practice about two decades ago [21-23]. A series of investigations in the field of artificial enzymes, fluorescent probes and molecular light emitting diodes were conducted on its background [24].

First unsubstituted structurally rigid analogs of 2,6-distyrylpyridine were synthesized in the late 1970s [25,26], then some of them were used as semi-products in organic synthesis [27,28], recently the series of their pyrazolic analogs was synthesized [29]. Generally, scientific investigations of this class were still limited to the evaluation of their physiological activity [30]. Taking into account high analytical potential of this class, a series of the simple derivatives was synthesized [31,32] with the purpose of studying their molecular structure and fluorescent properties. Protolytic interactions of a few representatives of this class were investigated as well [33].

The 2,6-distyrylpyridine analogs are the molecules with the cross-conjugated π-system, they are characterized by rather high fluorescence quantum yields with fluorescent parameters strongly depending upon the nature their microenvironment. High synthetic accessibility of the new compounds of this class with the increased length of their π-conjugated system and substituents of different electronic origin allow designing of the new multi-purpose fluorescent sensing materials on their background [16]. The main focus of the present paper is the detailed investigation of the acid-base equilibria in the extended series of the structurally rigid analogs of 2,6-distyrylpyridine.

2. Experimental Procedure

2.1. Chemicals

The molecular structure of the structurally rigid analogs of 2,6-distyrylpyrydine, (3E,5E)-3,5-dibenzylidene-8-phenyl-1,2,3,5,6,7-hexahydrodicyclopentano[b,e]pyridine, (1–18) involved in the present study were shown in the Scheme 1. Their synthesis, physical parameters, structure elucidation and conformation analysis were previously described in detail [31].

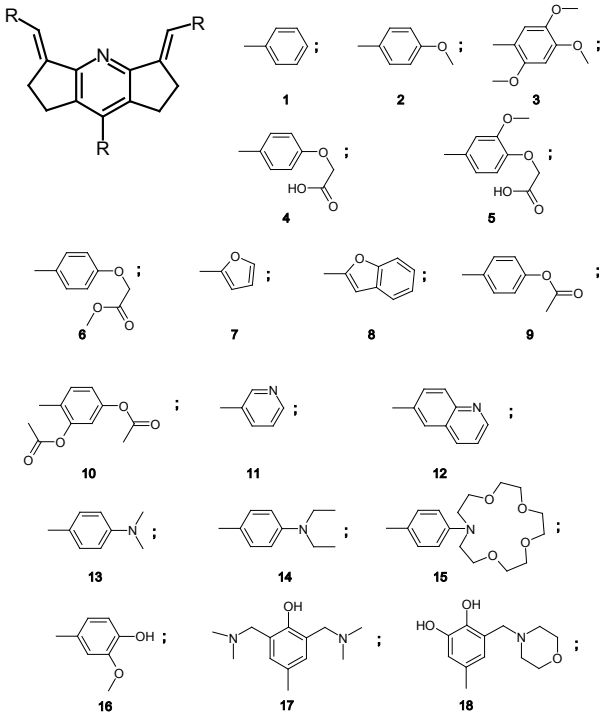

Scheme 1. Molecular structure of the investigated derivatives of (3E,5E)-3,5-dibenzylidene-8-phenyl-1,2,3,5,6,7-hexahydrodicyclopentano[b,e]pyridine, 1–18.

Specially purified ethyl alcohol [34,35] was used for the spectroscopic investigations.

Fluorescein in the bicarbonate buffer solution with pH=9.93 (quantum yield, φ_f = 0.85 [36]) and quinine bisulfate in 0.1N H_2SO_4 (φ_f = 0.546 [37]) were used as the fluorescence quantum yield reference standards. Difference in refraction indices of the investigated and the reference solutions was taken into account at estimation of fluorescence quantum yields [36].

2.2. Procedure

Electronic absorption spectra were measured on the Hitachi U3210 spectrophotometer, fluorescence spectra and quantum yields – on Hitachi F4010 fluorescence spectrometer at concentration of 1-18 compounds near 2×10^{-5} mol L^{-1} and the cell thickness of 1 cm in the isothermic conditions at t = 20±0.1°C.

Investigation of the photochemical activity were made by the method of the dosed irradiation of the dyes 2×10^{-4} mol L^{-1} solutions in the 1 cm spectrophotometric cell by the monochromatic light 406±2 nm (grating monochromator MDR-12, LOMO, S.-Petersburg, Russia) of the 250 W high pressure Hg lamp (DRSh-250) collected and focused by the system of quartz lenses. After exposure during the given time intervals (from several seconds to tens of minutes) the electronic absorption and fluorescence spectra of the samples were measured.

Protolytic equilibria constants were estimated in the water-ethyl alcohol (80%$_{mass}$) mixtures, which pH values were controlled by the universal ionometer EV-74 equipped with the glass electrode ESL-11G-05, calibrated by the standard water buffer solutions. Interphase potential influence in the mixed solvent ethanol-water system was accounted by the correction of the experimental pH values on –0.11 units according to [38].

Acid-base spectrophotometric titrations were made for the series of solutions of the investigated dyes with the initial concentration of 2×10^{-5} mol L^{-1} and necessary amount of sulfuric acid or potassium hydroxide for the creation of pH values with the step of approximately 0.5 pH units. The intermediate pH values were produced by the mixing of the neighboring initial solutions.

2.3. Data treatment and analysis

Estimation of the effective equilibrium constants of protolytic interactions was made by the spectrophotometric/spectrofluorimetric titration data analysis using specially developed software, which realizes Fletcher-Powell algorithm for the non-linear iterative least squares procedure [39,40]. Up to 20-25 analytical wavelengths within the long-wavelength absorption or fluorescence bands were involved in the analysis. All the obtained wavelength-dependent pK values were averaged with the weight factors built on the base of the mean square errors at the given analytical wavelength.

Deconvolution of the experimental spectra into the individual absorption/emission bands was performed using specialized software, which realizes algorithm of the non-linear least squares and approximation of the individual band shape by the log-normal function proposed in [41].

Quantum-chemical modeling were made by the semiempirical PM6 method [42], included in the software package MOPAC2009 [43].

3. Results and Discussion

3.1. Protolytic interactions of the dyes 1–8 possessing only one reaction center

Typical changes in the absorption and emission spectra of the investigated compounds as the pH was decreased are connected with the protonation of their main basic center – pyridine nitrogen atom (Fig. 1).

The pyridine cycle in the title molecules plays the role of the electron withdrawing unit, thus the electronic excitation in the investigated series of compounds is

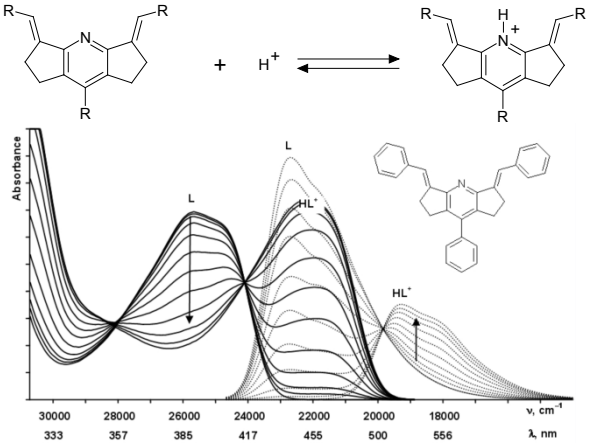

Figure 1. Changes in the absorption (solid lines) and fluorescence spectra (dashed lines) of compound 1 at its acid-base titration at pH from 8 down to 0.5

accompanied by the electron density removal from the side phenyl moieties towards the pyridine nucleus [44]. Protonation of the lone electron pair of the pyridine nitrogen increases the above feature and determines the observed red shifts both in the absorption and emission spectra. Substituents introduced in the side benzene rings regulate the electron density movement and spectral shifts according to their electron donor origin (Table 1). For example, protonation-induced bathochromic shift in the absorption spectra of 1 is nearly 3500 cm^{-1}, while as for the 4'-OCH_3-substituted compound the analogous shift is of 4280 cm^{-1}. Weaker donors in the dyes 4–6 are responsible for the intermediate spectral effects 3900–4000 cm^{-1}, while as the most prominent shift (4740 cm^{-1}) was observed for compound 3 having three OCH_3 substituents in each side benzene ring.

Fluorescence spectra of compounds 1-8 demonstrated analogous tendency, however, it is worth noting the lower red shifts of the emission bands at protonation. This is the reason of the generally lower Stokes shifts registered for the protonated forms of the dyes 1-8 in comparison to that of the neutral ones. The increased fluorescence Stokes shift of the ground state non-planar molecules in many cases indicated their excited state planarization [45-48]. In this course the decrease of the Stokes shifts of the 1-8 protonated forms could be interpreted as the consequence of definite planarization of their molecules at proton binding. The correlation between Stokes shift decrease and the electron donor ability of substituents in the side benzene rings supports this statement indirectly: compare the decrease of $\Delta\nu_{ST}$ at protonation for 1 (100 cm^{-1}) and 3 (720 cm^{-1}).

The results of our quantum-chemical calculations supported the above suggestions. According to them, the protonated forms of 1-8 should be more planar in

their ground state in respect to the neutral ones. The PM6-simulated angle between the side benzene ring belonging to the styryl moiety and the central pyridine cycle of 1 should be near 68º [44], while as for 1·H⁺ this angle decreases to 60º. Thus, the most planar in the discussed 1-8 subseries should be the protonated form of 3, for which the discussed angle falls down to 30°.

Generally, pyridine should be protonated rather easily. In water its log K_b=4.94 [49], while in methyl alcohol this value is only a little higher log K_b=5.21. In this study, protolytic interactions were investigated in the water-ethanol system (20:80) (Table 1), however, all of the equilibrium constants are significantly lower than that of pyridine [49]. The enlargement of π-conjugated system should increase proton affinity, however the results reported in [50] demonstrate the opposite tendency for 2,6-distyrylpyridine (log K_b=4.3, acetonitrile-water) and its heterocyclic analogs. For our compound 1, which is the iso-π-electronic analog of 2,6-distyrylpyridine, the basicity decrease is even more significant (log K_b=2.81). The above facts could be explained by examining the steric effects in the investigated compounds. Thus, decrease of 2,6-distyrylpyridine basicity instead of expected increase indicates the steric shielding of the pyridine ring nitrogen atom by the styryl moieties in positions 2 and 6 (Scheme 2b – the most sterically favorable to proton binding conformation is shown). The steric accessibility of the protonation center further decreases with the structural fixing of styryl moieties by the saturated carbon chains in the molecule of 1 and the other title compounds (Scheme 2a).

Protolytic equilibria constants (Table 1) demonstrate clear correlation with the nature of substituents in the side arylidene fragments. The lowest basicity is typical

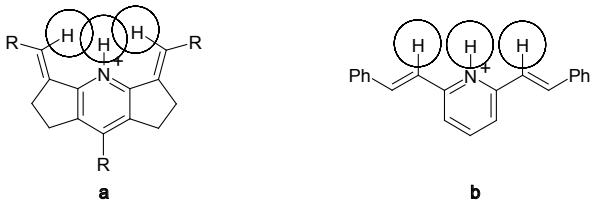

Scheme 2. Spatial accessibility to protonation of the pyridine nitrogen atom in the series of the dyes 1-18 (a) and model 2,6-distyrylpyridine (b).

to compound 8 with R=benzofuryl. Increasing of the electron donor properties of the R groups resulted in the increase of basicity. According to the data of [14] increase of the pyridine nitrogen partial electric charge on 0.01e should result in the increase of K_b approximately on 1 logarithmic unit. However, we did not find satisfactory correlation (r^2≈0.7) between the quantum-chemically calculated pyridinic nitrogen charges in the series 1-8 and the experimental log K_b values. Such discrepancy may be the result of the steric effects, which dominate over the electronic ones in the studied series.

The excited state basicity constants estimated on the background of the fluorescence titrations data are generally higher (approximately 1 logarithmic unit with the exception of compound 3) reflecting the increase of the intramolecular donor-acceptor interaction in the excited molecules.

For all the discussed compounds 1-8 the titration curves demonstrated much better fitting in the two-step interactions model in comparison with that of single-step one, which should be applied for single proton binding center species (Fig. 2, the data treatment correlation coefficients for 1 were 0.999 for two-step protonation model and 0.954 for the single step one). Such behavior

Table 1. Spectral and protolytic parameters of compounds 1-8.

Compound	Protolytic form	Absorption spectra		Fluorescence spectra			
		ν, cm⁻¹(λ, nm)	log K_b	ν, cm⁻¹(λ, nm)	$\Delta\nu_{ST}$, cm⁻¹	ϕ_f	log K_b
1	L	25660(390)	2.81±0.02 (EE)	22680(441)	2980	0.36	3.81±0.02(EE)
	HL⁺	22160(451)	1.61±0.01 (EZ)	19280(519)	2880	0.25	2.11±0.03(EZ)
2	L	24820(403)	3.77±0.01 (EE)	21080(474)	3740	0.28	4.41±0.04(EE)
	HL⁺	20540(487)	2.70±0.01(EZ)	17280(579)	3260	0.16	3.35±0.09(EZ)
3	L	24260(412)	3.95±0.01 (EE)	19240(520)	5020	0.44	3.98±0.01(EE)
	HL⁺	19520(512)	2.73±0.02(EZ)	15220(657)	4300	0.011	3.23±0.05(EZ)
4	L	24980(400)	3.42±0.01 (EE)	20920(478)	4060	0.39	3.51±0.03(EE)
	HL⁺	21040(475)	2.54±0.01(EZ)	17580(569)	3460	0.25	2.67±0.08(EZ)
5	L	24540(407)	3.68±0.01 (EE)	20400(490)	4140	0.23	3.95±0.01(EE)
	HL⁺	20640(484)	2.86±0.01(EZ)	16800(595)	3840	0.083	3.08±0.02(EZ)
6	L	25020(400)	3.65±0.01 (EE)	21160(473)	3860	0.36	3.88±0.02(EE)
	HL⁺	21020(476)	2.89±0.01(EZ)	17440(573)	3580	0.12	3.12±0.05(EZ)
7	L	22980(435)	3.23±0.02 (EE)	20300(493)	2680	0.37	4.07±0.03(EE)
	HL⁺	19220(520)	2.42±0.03(EZ)	16720(598)	2500	0.19	3.09±0.01(EZ)
8	L	21980(455)	2.40±0.07 (EE)	19360(517)	2620	0.65	3.48±0.05(EE)
	HL⁺	18340(545)	1.09±0.07(EZ)	15720(636)	2620	0.23	2.13±0.02(EZ)

Here L denotes the free base (free ligand), HL⁺ - its mono-protonated form; K_b denotes the equilibrium dissociation constant of the conjugated acid (HL⁺) – common quantitative measure for the basicity of the weak organic base (L)

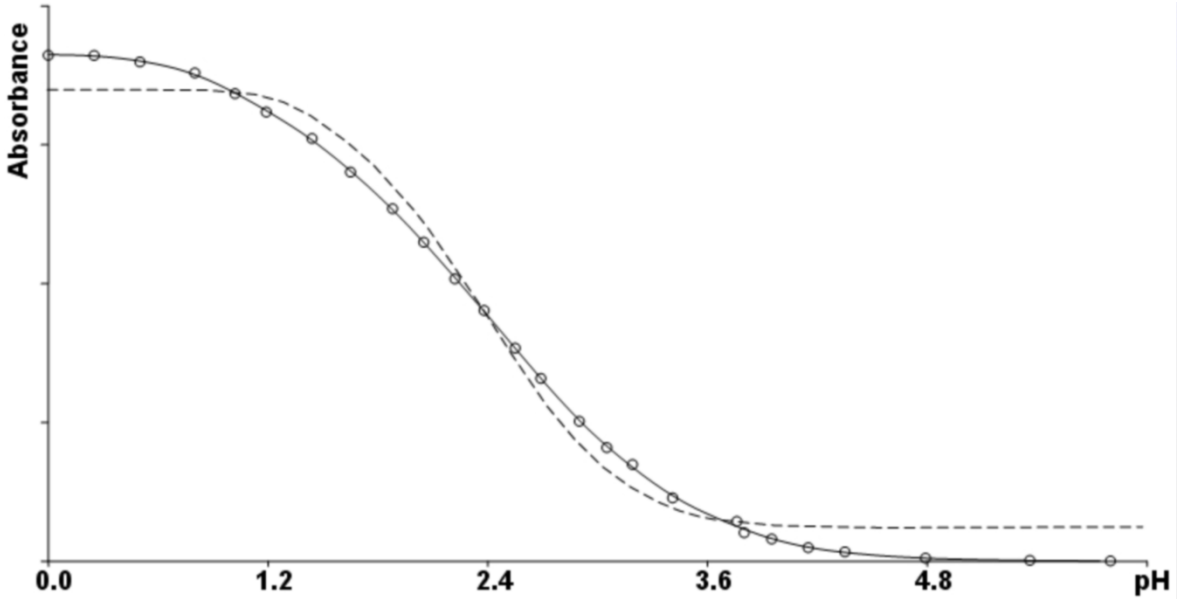

Figure 2. Mathematic treatment of the data of spectrophotometric titration of compound 1 at its protonated form long-wavelength absorption maximum. Circles – experimental data points, dashed line – single-step interaction model (log K_b= 2.5), solid line – two-step interaction model (log K_{b1}=2.8, log K_{b2}=1.6)

could be explained at assuming the existence of two different forms independently interacting with protons in acidic solutions.

As it was reported earlier [51], derivatives of 2,6-distyrylpyridine are able to effective photochemical E→Z isomerization around their C=C double bonds. Upon UV/Vis irradiation into the long-wavelength absorption bands, the studied compounds demonstrate spectra changes typical to the formation of the products with significant violation of π-conjugated system planarity. Taking into account the presence of two potentially photoactive double bonds, we can suggest the multi-step photochemical transformations EE → EZ → ZZ (Scheme 3).

The absorption spectra of corresponding marginal forms obtained at irradiation of compound 1 in ethanol solution are shown on the Fig. 3. All photogenerated species absorb light in the blue region compared to that of the initial EE, the general spectra shape of EE and EZ does not differ significantly one from another.

The photoisomerization velocity depends strongly on the polarity and proton donor ability of the solvent

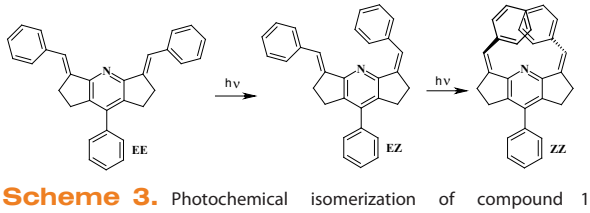

Scheme 3. Photochemical isomerization of compound 1 in solutions.

[51]. The first phototransformation stage EE→ EZ needed several minutes of irradiation in ethanol, while formation of the ZZ-isomer was much slower and required continuous irradiation during 6-8 hours. Thus, at synthesis, purification, storage and solutions preparation of the investigated compounds without special precautions against their solar or laboratory lamps illumination, definite amount of the "rapid" EZ-isomer could be formed in the experimental samples and/or solutions prepared for spectrophotometric experiments. This is the possible reason of the appearance of the second component independently interacting with acid at the above described titration studies.

Accounting of the two parallel equilibria results in two protolytic constants differed significantly one from another. Compound 1 demonstrated two proton binding equilibria with log K_b 2.81 and 1.61 (Table 1), which should be attributed to its EE and EZ forms correspondently. Decrease of proton affinity in the case of EZ isomer could be the consequence of the additional steric shielding of the protonation center by one of the structurally fixed styryl moieties in Z configuration. The electronic factors act in agreement with the steric ones: PM6 method calculated ground state negative charges on the pyridine nitrogen atom for the photoisomers of compound 1 were the following: –0.285 (EE) and –0.275 (EZ). The most significant difference in the protonation constants was registered for compound 8, which side group spatial dimensions were the greatest within the examined series 1-8.

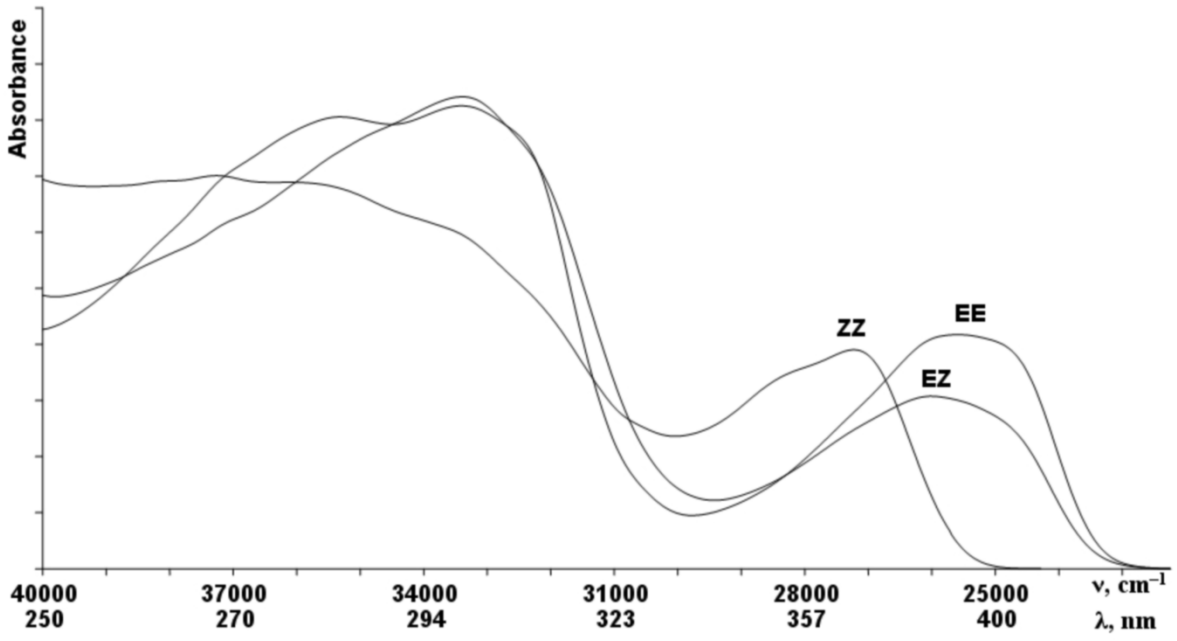

Figure 3. Absorption spectra of EE, EZ and ZZ isomers of 1 in ethyl alcohol, obtained at irradiation at 406 nm of the 250 W high pressure mercury

The additional experiment was conducted to confirm our hypothesis concerning the parallel protonation processes of the mixture of photoisomers. Preliminary irradiation of the water-ethanol solution with sufficient dose converted all EE to EZ isomer, but too low to generate detectable concentration of ZZ one, results in the single-step spectrophotometric titration curve with the lower equilibrium constant initially attributed to EZ form of 1. Thus, basing on the described results we could consider the photochemical E→Z isomerization of the basic organic compounds as a tool for the widening of their titration interval owing to the presence of the two photoisomers titrated independently one from another and differed by their protolytic constants at least on 1 logarithmic unit.

3.2. Protolytic interactions of compounds 9-15 with several potential proton-binding centers

Compounds 9-15 were classified in the separate subseries owing to the realization of several protolytic equilibria connected not only with the proton binding to the nucleophilic pyridine nitrogen, but also to the other functional groups introduced into the side benzene rings as substituents.

Compounds 9-10 behave similarly to those discussed early: protonation of their pyridinic nitrogen was observed in the pH range 4 to 1 with two equilibrium constants, which we attributed to the coexistence of their EE and EZ photoisomers. Generally 9-10 are weaker bases (Table 2) in comparison to 1-8, owing to the weak electron accepting nature of their acetoxy substituents. Difference in basicity of their EE and EZ forms are more significant in comparison with the previously discussed subseries, that is why we succeeded to detect individual spectral parameters of the protonated forms for these photoisomers (Fig. 4, Table 2).

It is worth noting that spectral and protolytic parameters of EE isomers of 9-10 are quite similar, which is the indication of the low influence of acetoxy group in meta'-position of their side benzene rings. The most pronounced difference was detected for the protonation of the EZ-form, which is substantially hindered by the additional substituents in the molecule 10. The analogous tendency was observed for compound 8 as well. The only principal difference should be underlined for 9-10 in respect to 1-8: increasing of the fluorescence Stokes shifts for the protonated EZ-isomers. The possible reason of such behavior could be the less rigid molecular structure of mono-cation owing to the electron accepting nature of the introduced substituents, which decreases intramolecular donor-acceptor interactions.

At higher acid concentration range (which corresponds to Hammet acidity function H_0 [52]) one more additional protolytic form appeared. It could be connected only with the protonation of one of the acetoxy groups, the obtained equilibrium constant value supported this hypothesis: the benzoic acid esters and phenol esters of aliphatic acids are being protonated in the H_0 range –7.3 to -7.8 [53], this value is close to the

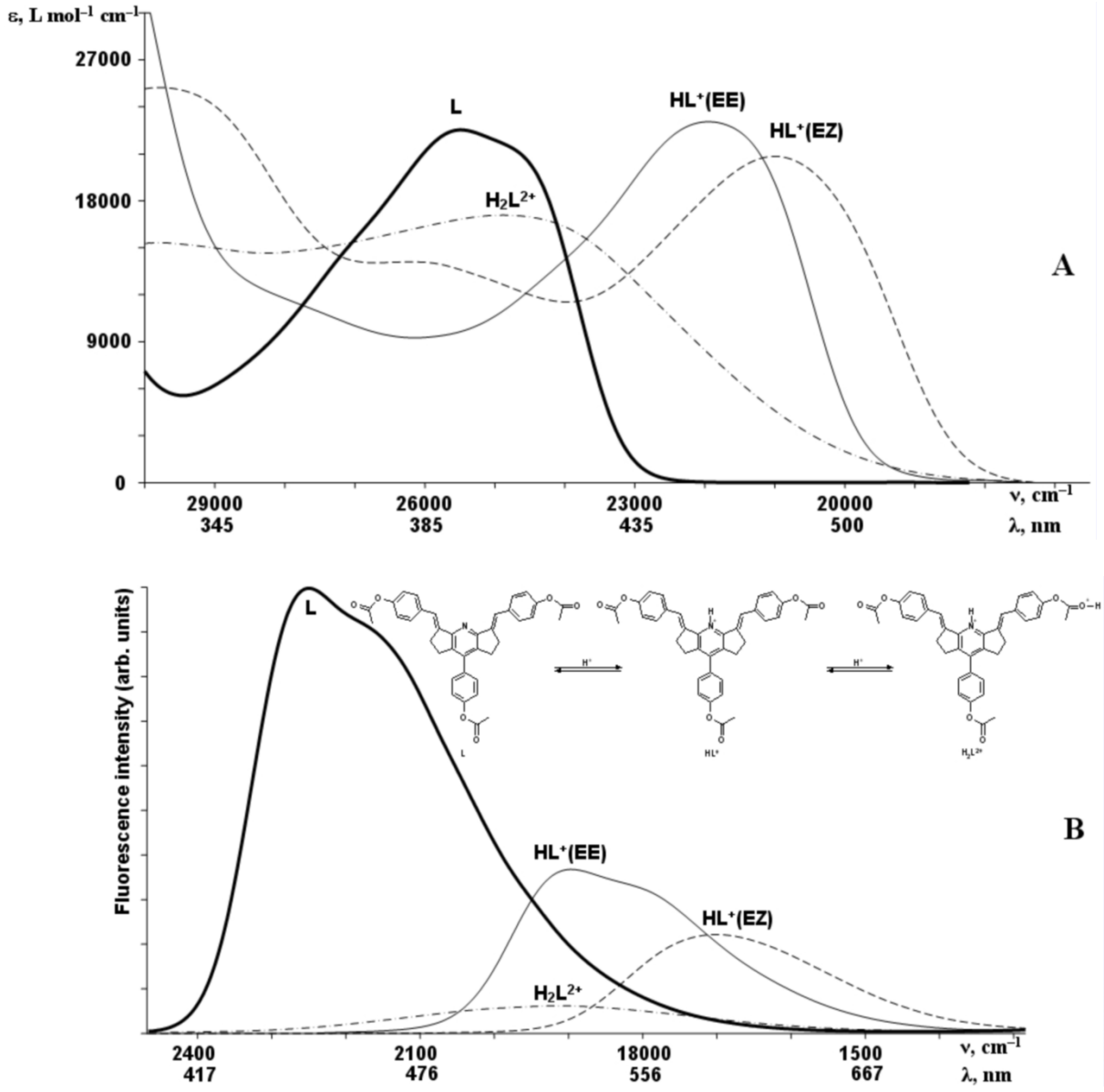

Figure 4. Electronic absorption (A) and fluorescence (B) spectra of the observed protolytic forms of compound 9.

Table 2. Spectral and protolytic parameters of compounds 9 and 10.

Compound	Protolytic form	Absorption		Fluorescence			
		ν, cm⁻¹(λ, nm)	log K_b	ν, cm⁻¹(λ, nm)	$\Delta\nu_{ST}$, cm⁻¹	ϕ_f	log K_b^*
9	L	25540 (392)	–	22480 (445)	3060	0.352	–
	HL^+ (EE)	21980 (455)	2.42±0.02	18900 (529)	3080	0.206	2.44±0.08
	HL^+ (EZ)	21020 (476)	1.05±0.09	17000 (588)	4020	0.112	0.45±0.08
	H_2L^{2+}	24880 (402)	–7.73±0.04	19140 (522)	5740	>0.001	–7.5±0.1
10	L	25560 (391)	–	22540 (444)	3020	0.256	–
	HL^+ (EE)	21860 (457)	2.42±0.02	19180 (521)	2680	0.097	2.35±0.08
	HL^+ (EZ)	20120 (497)	0.76±0.09	16500 (606)	3620	0.025	0.19±0.05
	H_2L^{2+}	24640 (406)	–7.77±0.04	18560 (539)	6080	>0.001	–7.6±0.1

high acidity range acid-base equilibrium constants of 9-10.

Protonation of the side acetoxy group results in the significant hypsochromic shifts, because proton binding increases the electron withdrawing ability of such substituent. Doubly protonated forms of 9-10 are characterized by the increased up to ~6000 cm^{-1} fluorescence Stokes shifts, most pronounced for the di-cation of compound 10. It is not possible to elucidate correctly the C=C bonds configuration of the doubly protonated 9-10, thus their high media acidity range equilibrium constants should be considered as the averaged ones.

The molecules of compounds 11-15 are characterized by the presence of four proton accepting centers. Owing to this fact their protolytic equilibria are much more complicated. Let us note that in the cases of 11-15 (and several further considered compounds of the investigated series) it was not possible to distinguish the individual protolytic equilibria for the photochemically generated isomeric forms (EE/EZ/ZZ). Therefore, all the protolytic constants for them presented in this paper should be considered as the averaged values.

Compounds 11-12 include correspondently pyridine and quinoline moieties. Their nitrogen atoms are not in the well-conjugated positions with the central pyridine nucleus, the most important part of the chromophore fragment of the title compounds. That is why they do not significantly influence the spectral parameters of 11-12. Moreover, spectral changes related to protolytic interactions were rather insignificant for these compounds (Fig. 5). All four pyridine nitrogen atoms of compound 11 carried approximately the same electric charges of approximately –0.29e (PM6 calculations). That is why the probability of their protonation should be similar one to another. To identify the nature and sequence of the multi-step protolytic interactions for this compound, we made a series of model quantum-chemical calculations of their mono- and poly-protonated cationic forms (Table 3). The same approach was applied to compound

Table 3. Heats of formation (kcal mol^{-1}) of various protolytic forms of compounds 11 (upper value) and 12 (lower value) calculated by the method PM6

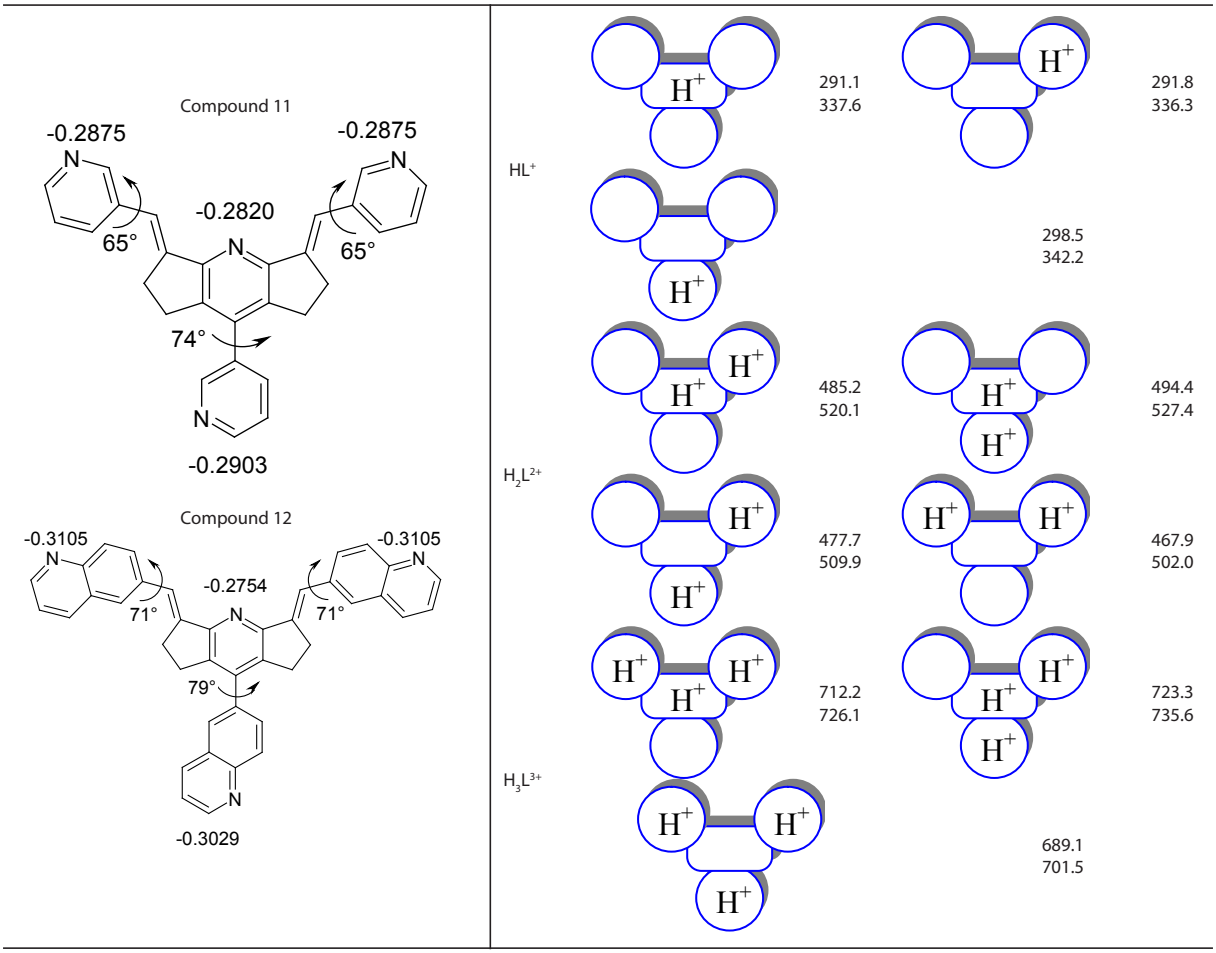

12, which should be characterized only by a small increased electronic asymmetry.

According to the modeling presented in Table 3, for the first step of acid-base interactions of 11-12 the less probable protonation is the proton binding to the heterocycle in position 4 of the central pyridine moieties. The other nucleophilic centers should demonstrate nearly the same proton accepting activity. At the second stage the di-cationic form with both side heterocyclic units seem to be the most favorable. Even at the next stage of interactions, protonation of the central pyridine nitrogen atom was not expected according to the results presented in the Table 3.

Basing on the above data and considerations one could propose the sequence of protonation steps for compound 11 and similarly to 12 presented in the Scheme 4.

The proposed order of proton binding does not contradict the protonation-related changes observed in the absorption spectra of compound 11 (Fig. 5). In the rather wide pH interval from 8.5 to 2, a delicate alteration in the bands shape and positions were observed both in the absorption and in the fluorescence spectra. Side pyridine cycles do not significantly influence the main chromophoric unit of this molecule owing to its unplanarity. Identification of the individual equilibria was possible only at analysis of the positions of the observed isosbestic points and elucidation of their existence pH ranges, presented on the Fig. 5.

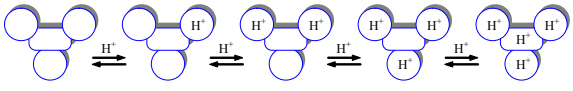

Scheme 4. The possible general sequence of stages for the protolytic interactions of compounds 11 in the acidic media

The dramatic red shift in the absorption spectra indicated the proton attachment to the nitrogen atom of the central pyridine unit only in the highly acidic media. Fluorescence spectra were so insensitive to protonation, that identification of only the H_4L^{4+} species was possible with their help.

Analogous tendencies in the absorption spectra of compound 12 at its protonation are expressed a little more substantially because of its longer conjugated system. According to the values of protonation constants close to those of pyridine and quinoline, the side heterocyclic unit nitrogen atom was involved in the interactions on the first stage (Table 4). Second proton attachment to one of the other potential reactive centers was hampered by the presence of positive charge in the molecule. Surprisingly, the basicity of compound 12 was lower compared to that of 11 for all the stages of interactions despite higher electrical charges on the nitrogen atoms predicted by quantum-chemical calculations and general higher basicity of quinoline in respect to pyridine.

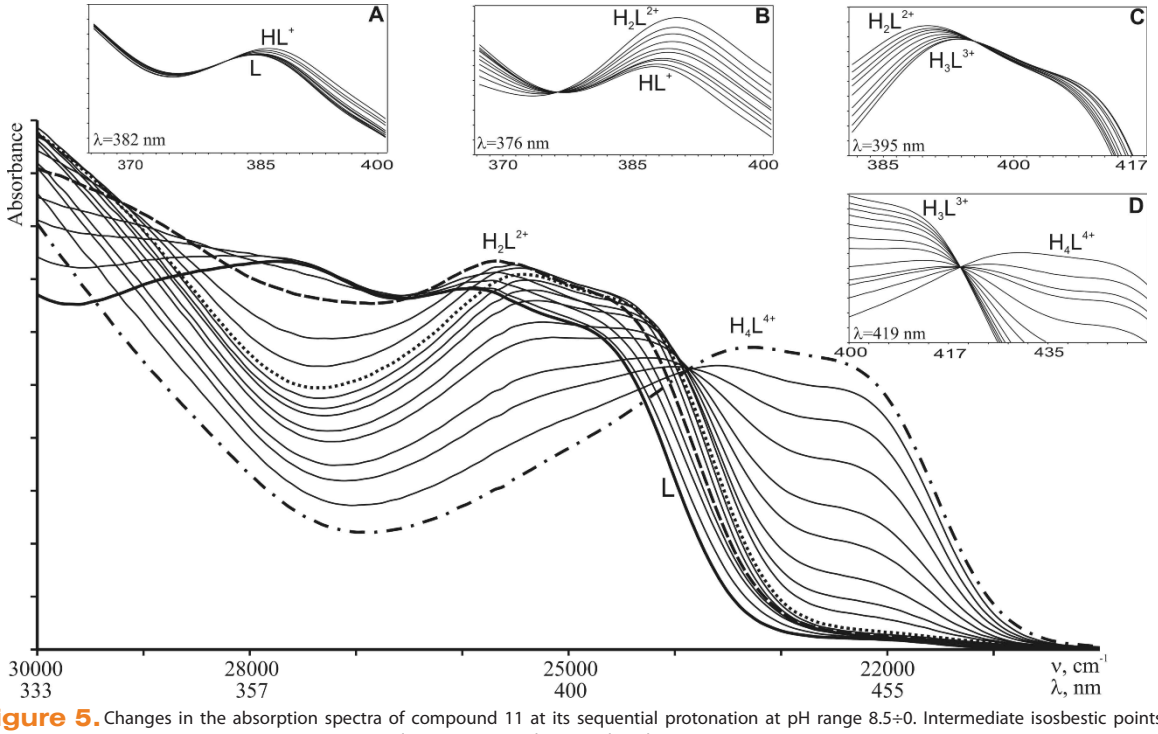

Figure 5. Changes in the absorption spectra of compound 11 at its sequential protonation at pH range 8.5÷0. Intermediate isosbestic points at 382 nm (A), 376 nm (B), 395 nm (C) and 419 nm (D) are shown in the inlays.

Table 4. Spectral and protolytic parameters of compounds 11 and 12.

Compound	Protolytic form	Absorption		Fluorescence		
		ν, cm^{-1}(λ, nm)	log K_b	ν, cm^{-1}(λ, nm)	$\Delta\nu_{ST}$, cm^{-1}	ϕ_f
11	L	25920 (386)	–	22900 (437)	3020	0.13
	HL^+	25840 (387)	5.4±0.2	–	–	–
	H_2L^{2+}	25660 (390)	3.98±0.01	–	–	–
	H_3L^{3+}	25420 (393)	2.44±0.03	–	–	–
	H_4L^{4+}	23220 (431)	0.97±0.06	20440 (489)	2780	0.16
12	L	26040 (384)	–	21860 (457)	4180	0.38
	HL^+	25640 (390)	5.2±0.1	–	–	–
	H_2L^{2+}	23420 (427)	3.85±0.02	–	–	–
	H_3L^{3+}	22540 (444)	1.51±0.02	–	–	–
	H_4L^{4+}	22220 (450)	0.72±0.01	19300 (518)	2920	0.12

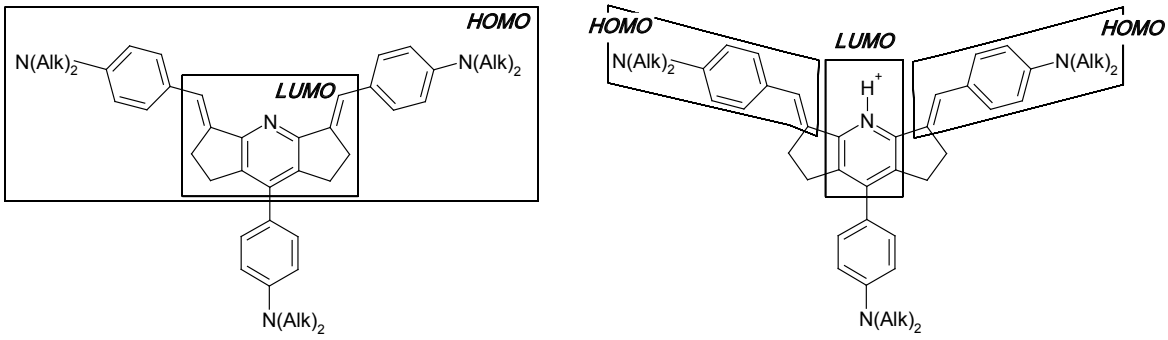

Scheme 5. Localization of the boundary molecular orbitals in the neutral and mono-cationic forms of compounds 13-15.

The strong electron donor dialkylamino groups are attached to the main chromophore fragment of compounds 13-15. This changes the nature of the long-wavelength electronic transitions in their electronic absorption spectra to "transitions with substantial intramolecular charge transfer" [44] owing to the dramatic difference in localization of their boundary molecular orbitals (Scheme 5). The discussed substituents could be easily protonated in moderately acidic media, which is why we also expected principal changes in the scheme of acid-base interactions of 13-15 in comparison with those of 11-12.

Substantial long-wavelength shift on ~5500 cm^{-1} was observed for compounds 13-15 even in the weakly acidic media (the data for compound 14 is shown on the Fig. 6), during which only one proton binds to the studied molecule according to the mathematical treatment of titration data in this pH range.

All the arguments pointing out the most probable protonation center in this case is the central pyridine nucleus nitrogen atom. First, N,N-diethylaniline is less basic then pyridine in water and in methanol solutions [54]. Second, our quantum-chemical calculations revealed the pyridinic nitrogen atom (marked by the letter a on the Fig. 6) as the most negatively charged center in these molecules. Mono-cations with protonated pyridine nitrogen are the most energetically favorable ones for the 13-15 subseries according to our PM6 method modeling. Third, the bathochromic shift in the electronic spectra should be observed only in the case of pyridine nitrogen protonation. Otherwise, proton binding to the dialkylamino-group should result in the excluding of its lone electron pair from the conjugation with the π-system of the neighboring benzene ring which induces pronounced hypsochromic effect. Several publications reported protonation of pyridine nitrogen atom prior to the dialkylamino-group in the cases of their occurrence in the same molecule, for example, [55].

The intramolecular charge transfer (see Scheme 5) in molecules 13-15 at electronic excitation [44] should be significantly enforced at protonation of their pyridine nitrogen atom. This fact gave rise also the distinct appearance of Kiprianov-like splitting of the long-wavelength absorption band [56]. The well-resolved doublet of the absorption bands (494 and 580 nm) is clearly observed in the spectrum of mono-cationic form of 14 (HL^+, Fig. 6). Two other discussed dialkylamino derivatives behave similarly.

Further pH decreases of the media resulted in protonation of one of dialkylamino groups marked in the Fig. 6 by letters b or c. Protonated dialkylamino-substituents lose its electron donor ability and became weak acceptor acting in the framework of the inductive effects only. Quantum-chemical calculations predict twisting of the protonated side $NHAlk_2^+$-styryl fragment on the angle of near 70°, which significantly excludes

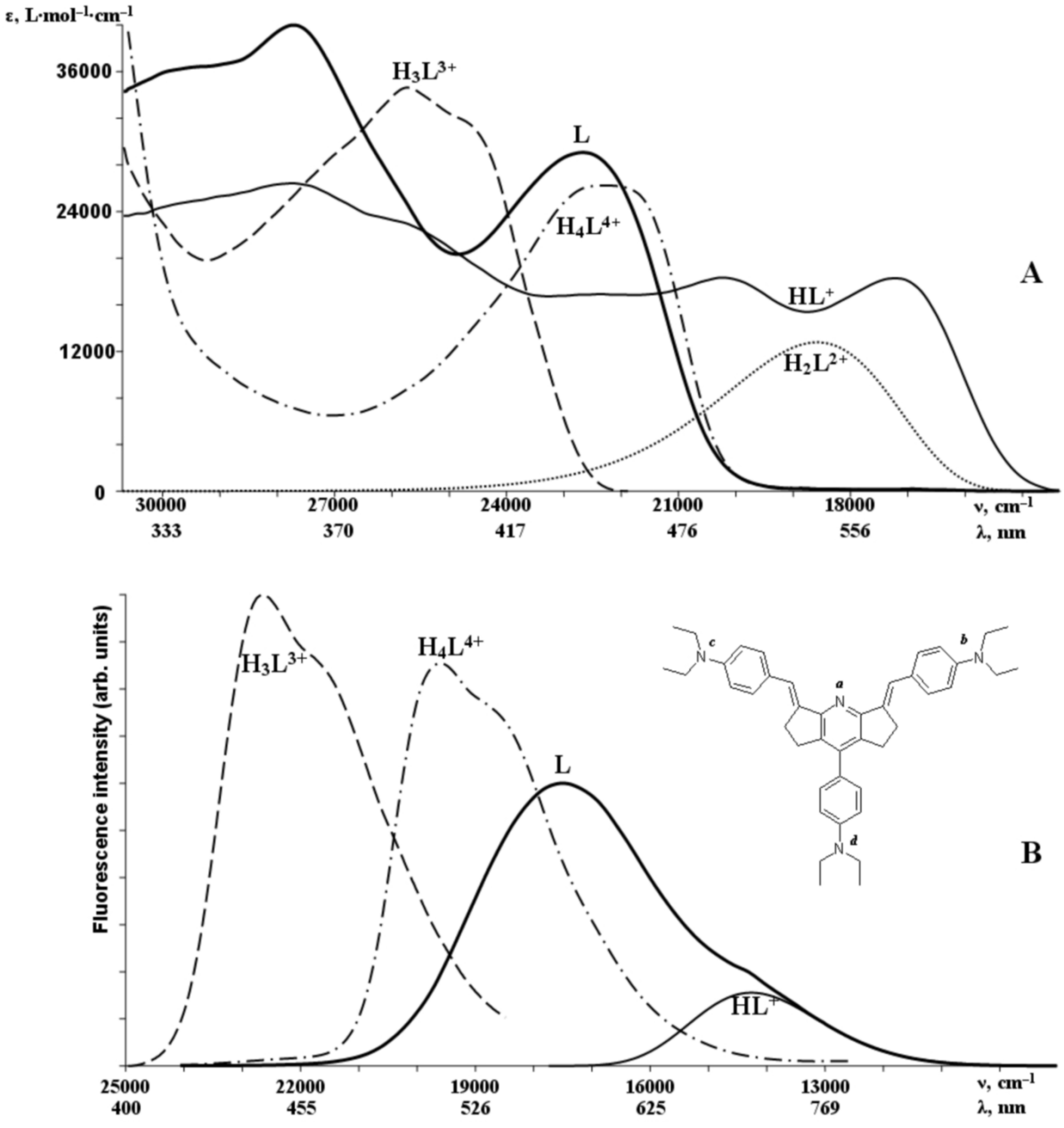

Figure 6. Absorption (A) and fluorescence (B) spectra of different protolytic forms of compound 14. Only the long-wavelength absorption band extracted from the experimental spectra by the procedure of deconvolution is presented here for the di-cationic form H_2L^{2+}.

it from the conjugation with the main chromophore of the molecule. All these features lead to the disappearing the Kiprianov-like splitting [56] of the long-wavelength absorption band. The H_2L^{2+} form absorption band was observed approximately between the components of the splitted doublet of the mono-cationic form (Fig. 6). This is the indication of the symmetry breaking in the corresponding protonated form – the main reason for the above mentioned absorption band splitting.

Attachment of the third proton was accompanied by substantial hypsochromic shift in the absorption spectra of 13–15 on ~7000 cm^{-1}, while as the last bound proton induced significant batochromic effect (~2000 cm^{-1}). It seems to be logical to assume the attachment of the third proton to the site c or, less probable, d (notation of the Fig. 6) taking into account the occupation of the sites a and b in the dicationic form. Describing the substantial blue shift in the absorption spectra of 13-15 the proposed sequence of stages could not, however, clarify the following red shift. Moreover, all the already discussed bathochromic effects were usually connected with the protonation of the central pyridine nitrogen,

which had already been protonated in HL^+ and H_2L^{2+}.

To resolve the situation we made an assumption that third protonation initiated the tautomeric rebuilding of the formed particle H_3L^{3+} with removing of proton from site a and binding it to d. This could be the synchronous process via the chain of the solvent/acid molecules or the sequential one with dissociation of H_3L^{3+} site a and subsequent proton binding to d. To confirm this statement we made quantum-chemical calculations of all the possible isomeric three-cationic structures with the aim to find out the most energetically favorable among them (Scheme 6).

Indeed, the most thermodynamically stable was the b,c,d form of H_3L^{3+}. The mean energetic difference between this and the other three-cationic structures was near 10-15 kcal/mol, this is enough to be the driving force of the discussed tautomeric transformation aiming to deprotonate the central pyridine cycle and to make it ready for the attachment of the fourth proton on the next stage of acid-base interactions.

We would like to propose additional arguments in favor of the above hypothesis. The electronic absorption spectra of protonated dialkylamino compounds are generally very similar to those of unsubstituted molecules. This is because the NH^+Alk_2-group is not capable of the mesomeric effects so important to electronic spectroscopy, and influences the spectra only as definite perturbation factor. In this connection, the last stage of protonation of compounds 13-15 should be very similar in its spectral manifestation to that of the single-stage protonation of unsubstituted molecule 1. Direct analogy not only in position, but also in the shape of the experimental spectral curves, is clearly seen at comparison of the data of the Tables 1 and 5 / Figs. 2 and 6.

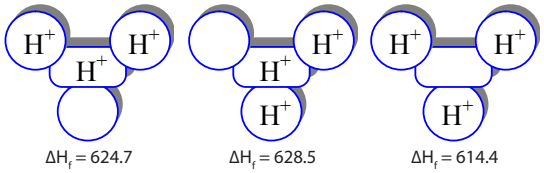

13 $\Delta H_f = 624.7$ $\Delta H_f = 628.5$ $\Delta H_f = 614.4$

14 $\Delta H_f = 587.9$ $\Delta H_f = 590.1$ $\Delta H_f = 580.9$

Scheme 6. Heats of formation (kcal mol^{-1}) of all the possible three-cationic forms of compounds 13 and 14.

The last evidence in favor of the proposed mechanism could be found in the spectral data for 13-15 presented in the Table 5. The electronic absorption and fluorescence spectra for neutral forms, HL^+ and H_2L^{2+} cations of 13-15 differ, owing to the different nature of alkyl radicals of their $NAlk_2$-groups (methyl for 13, ethyl for 14 and azacrown ether residue for 15). However, spectral parameters for their three- and tetra-protonated forms are practically the same. This should be because of the complete protonation of $NAlk_2$-groups of 13-15 in H_3L^{3+} and H_4L^{4+} cationic particles. The protolytic equilibrium constants for the last stage of protonation of these compounds are close as well. Thus, bathochromic shift on the last protonation stage $H_3L^{3+} + H^+ \rightarrow H_4L^{4+}$ should be interpreted as attachment of proton to the central pyridine cycle nitrogen atom deprotonated at formation of three-cationic species H_3L^{3+}.

Summarizing the above discussion we could propose the general mechanism for the protonation of compounds 13-15 in the acidic media (Scheme 7).

Electron donor properties of N,N-dialkylamino groups significantly regulate the acid-base equilibria constants. Thus, compound 13 has first stage log K_b value practically the same as for the unsubstituted pyridine (electronic effects of dimethylamino-groups

Table 5. Spectral and protolytic parameters of compounds 13-15.

Compound	Protolytic form	Protonated sites*	Absorption ν, cm^{-1} (λ, nm)	Absorption log K_b	Fluorescence ν, cm^{-1} (λ, nm)	Fluorescence $\Delta\nu_{ST}$, cm^{-1}	Fluorescence ϕ_f
13	L	–	23660 (423)	–	17460 (573)	6200	0.09
	HL^+	a	20200 (495)**	4.95±0.01	14420 (693)	5780	0.02
	H_2L^{2+}	a, b	19420 (515)	3.02±0.05	–	–	–
	H_3L^{3+}	b, c, d	25780 (388)	2.15±0.05	22800 (439)	2980	0.02
	H_4L^{4+}	a, b, c, d	22640 (442)	1.36±0.03	19800 (505)	2840	0.01
14	L	–	22680 (441)	–	17520 (571)	5160	0.11
	HL^+	a	19900 (503)**	5.82±0.01	14280 (700)	5620	0.06
	H_2L^{2+}	a, b	18600 (538)	4.08±0.03	–	–	–
	H_3L^{3+}	b, c, d	25740 (389)	3.43±0.04	22640 (442)	3100	0.46
	H_4L^{4+}	a, b, c, d	22300 (448)	1.46±0.01	19620 (510)	2680	0.21
15	L	–	22900 (437)	–	18180 (550)	4720	0.14
	HL^+	a	19980 (500)**	5.18±0.01	14380 (695)	5600	0.11
	H_2L^{2+}	a, b	18860 (530)	3.5±0.1	–	–	–
	H_3L^{3+}	b, c, d	25780 (388)	2.6±0.1	22800 (439)	2980	0.53
	H_4L^{4+}	a, b, c, d	22560 (443)	1.51±0.07	19840 (504)	2720	0.25

** notations according to the Fig. 6*

*** position according the center of mass of the long-wavelength absorption band*

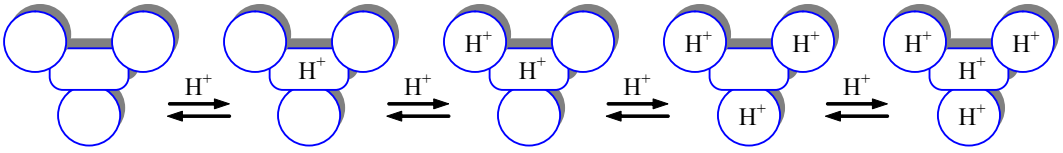

Scheme 7. Mechanism of protolytic interactions of compounds 13-15 in the acidic media.

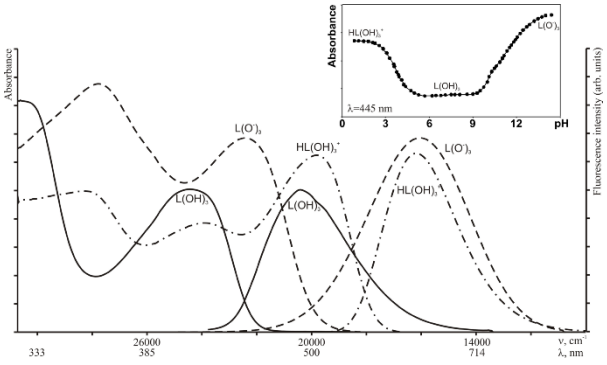

Figure 7. Absorption and fluorescence spectra of compound 16 and its protolytic forms. Plot of absorbency at 445 nm versus pH is shown in the inlay.

were compensated by the steric influence of structurally fixed styryl groups in positions 2 and 6 of the central pyridine moiety). The basicity of 14 is the highest within the discussed subseries, its log K_b=5.82 is close to the "physiological" pH interval [10].

3.3. Acid-base equilibria of compounds 16-18 possessing several protolytic centers of different nature

Compounds 16-18 include protolytic centers of both acidic and basic origin: pyridine cycle and aromatic hydroxy groups. That is why representatives of this subseries should demonstrate widest pH sensitivity interval among all the investigated compounds, which includes both acidic and basic ranges. First of them, 16, like most of the already discussed pyridine derivatives, is being protonated in the acidic media with the formation of mono-cation of the following composition $HL(OH)_3^+$ (Fig. 7). The observed spectral effects are typical to compounds 1-8 with only one protolytic center. Mathematical treatment of the titration data allows detecting the presence of photogenerated EZ-isomers in this case as well (Table 6).

Dissociation of hydroxy groups was observed in the basic media above pH ~ 9. However, on the contrary to protonation, difference in the spectral effects and dissociation equilibria constants were so insignificant in this case, that we failed to estimate individual absorption and emission spectra of various intermediate anionic species. The only final, three-anionic forms could be adequately characterized by their electronic spectra. Surprisingly, positions of emission bands for the protonated cationic form and fully dissociated three-anionic one were practically the same in the case of 16 (Fig. 7).

According to our data (Table 6) the acidity of OH-groups in 16 (pK_a = 9.2) is higher then that of phenol (pK_a = 9.95) and ortho-methoxy phenol (pK_a = 9.93) [53]. Second and third dissociation constants are logically lower because of the electrostatic interactions hampering each further dissociation stage for the formed anionic species (Table 6).

Protolytic interactions of 17 and 18 are much more complicated. As it was shown in [44], the excited state electron transfer from the aliphatic amine nitrogen towards the excited fluorophore moiety is typical to these compounds. This was reflected in the low fluorescence quantum yields of the neutral molecules and their various protolytic forms (Table 6). Space proximity of the proton donor hydroxy groups and proton accepting aliphatic nitrogen atoms (Scheme 8) significantly influenced the magnitude of their acid-base equilibrium constants. Probably, these groups are connected by the intramolecular hydrogen bonds, which facilitate dissociation. As it was shown in the Table 6, the OH groups of 17 and 18 are much more acidic in comparison to that of 16.

Moreover, protolytic interactions in the electronically excited state substantially differ from those in the ground state for the discussed compounds. Thus, dual fluorescence of the neutral forms of 17,18 observed in the pH interval 2.6 to 4.6 (Scheme 8, Fig. 8) reflects realization of the excited state intramolecular proton transfer reaction. The long-wavelength emission band was situated in the spectral range of mono-anionic form $L(OH)_2O^-$, supporting our hypothesis of OH group photodissociation. Protonation of trialkylamino-groups in the more acidic media decreases the probability of such proton phototransfer reaction down to its complete disappearing. In basic media, the surrounding photodissociation of OH groups is being realized by the intermolecular scheme with the participation of basic particles from the bulk of the solvent.

The most specific feature of the compounds 17 and 18 is the absence of conjugation between π-system of their main chromophoric fragments and tertiary amine lone electron pairs. Having practically negligible influence

Table 6. Spectral and protolytic parameters of compounds 16-18

Compound	Protolytic form	Absorption		Fluorescence		
		ν, cm^{-1}(λ, nm)	pK$_a$	ν, cm^{-1}(λ, nm)	Δν$_{ST}$, cm^{-1}	ϕ_f
16	$L(OH)_3$	24340 (411)	–	20420 (490)	3920	0.18
	$HL(OH)_3^+$	19820 (505)	3.78±0.01 (EE) 2.72±0.01 (EZ)	16200 (617)	3620	>0.01
	$L(O^-)_3$	22420 (446)	pK$_{a1}$ =9.2±0.1 pK$_{a2}$ =10.2±0.1 pK$_{a3}$ =12.1±0.1	16080 (622)	6340	>0.01
17	$L(OH)_3$	24720 (405)	–	21480 (466)	3240	0.025
	$HL(OH)_3^+$	20760 (482)	3.75±0.02 (EE) 2.55±0.03 (EZ)	17980 (556)	2780	>0.001
	$L(OH)_2(O^-)$	23780 (421)	5.28±0.08	16840 (594)	6940	0.05
	$L(OH)(O^-)_2$	24060 (416)	8.63±0.08	16180 (618)	7880	0.02
	$L(O^-)_3$	222220 (450)	13.32±0.02	16300 (613)	5920	>0.001
18	$L(OH)_3$	24540 (407)	–	20540 (487)	4000	0.05
	$HL(OH)_3^+$	20120 (497)	3.56±0.01 (EE) 2.59±0.02 (EZ)	16960 (590)	3160	0.04
	$L(OH)_2(O^-)$	24200 (413)	5.83±0.02	15660 (639)	8540	>0.001
	$L(OH)(O^-)_2$	24060 (416)	9.4±0.01	15100 (662)	8960	>0.001
	$L(O^-)_3$	22200 (450)	12.95±0.03	16160 (619)	6040	0.02

Here L(OH)$_n$ denotes multi-hydroxylic acid, which could bind proton(s) to form cationic species or undergo multi-step dissociation to form anionic species with corresponding dissociation equilibrium constant(s) K$_a$

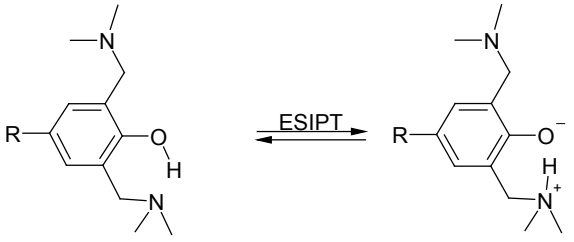

Scheme 8. Intramolecular hydrogen bonding and the excited state intramolecular proton transfer (ESIPT) in the molecules 17 and 18.

on the absorption spectra, these amine-containing substituents significantly influence fluorescence parameters. They decrease quantum yields owing to the electron transfer induced radiationless deactivation and enforce dissociative processes both in the ground and in the electronically excited states. The last circumstance causes continuous changes of their absorption and fluorescent parameters in the very wide pH range, from 0 to 14 (see inlays in the Fig. 8). This aspect makes compounds of the discussed subseries very prospective for creation on their background novel fluorescent pH sensing materials with extremely large analytically available interval and the possibility of ratiometric fluorescence detection [16].

4. Conclusions

Derivatives of the structurally rigid analogs of 2,6-distyrylpyridine - (3E,5E)-3,5-dibenzylidene-8-phenyl-1,2,3,5,6,7-hexahydrodicyclopentano[b,e] pyridine, take part in various acid-base interactions depending on their chemical structure and electronic nature of substituents in the side aromatics moieties.

Molecules with the only one protolytic center demonstrated significant long-wavelength shifts in their electronic absorption and fluorescence spectra. Basicity of the main proton binding center – pyridine nitrogen atom is regulated not only by the electronic factors,

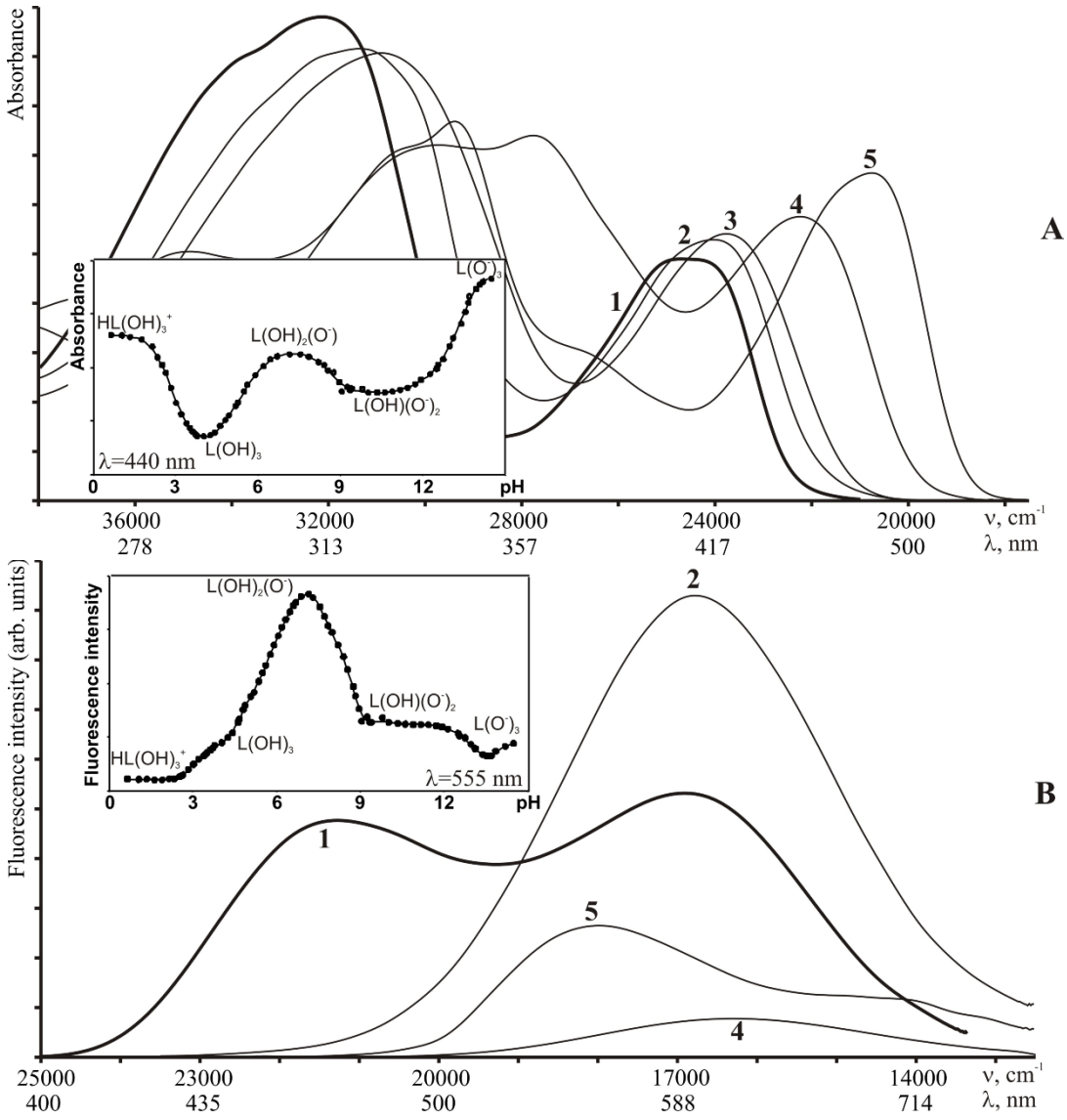

Figure 8. Absorption (A) and fluorescence (B) spectra of 17 and its various protolytic forms: 1 – $L(OH)_3$, 2 – $L(OH)_2O^-$, 3 – $L(OH)(O^-)_2$, 4 – $L(O^-)_3$, 5 – $HL(OH)_3^+$. Plots of the absorbance at 440 nm (A) and fluorescence intensity at 555 nm (B) versus pH are shown in the inlays.

but also by the steric effects of the substituents in the positions 2 and 6 of the pyridine cycle.

Owing to the effective photochemical E→Z isomerization, most of the investigated compounds exist in the mixture of their EE- and EZ-isomers, which are being protonated in different pH intervals. Thus, the coexistence of EE- and photogenerated EZ-forms could be considered as a factor of widening the pH detection range at the application of these compounds as fluorescent pH indicators.

Presence of several protolytic centers favors the diversity of acid-base interactions and further enlarges the pH sensitivity interval. Introduction of heterocyclic units with high proton affinity (pyridine, quinoline) gives rise to the appearance of the multi-step protonation sequences, at which the central pyridine cycle is being protonated only at the last stage. Dialkylamino-groups dramatically enforce the observed spectral effects both in the absorption and emission spectra further widening the pH sensitivity interval. For the last type of compounds the pyridine unit has been protonated at the first stage of interactions. Its temporal reprotonation (tautomeric rebuilding) was revealed between the 3 and 4 stages of proton attachment.

Introduction of substituents of both acidic and basic origin allowed widening pH sensitivity range of such compounds up to the complete pH scale from 0 to 14 units for the water and water-alcohol systems.

References

[1] R. P. Haugland, Handbook of Fluorescent Probes and Research Products, 9th edition (Molecular Probes Inc., Eugene, 2002)
[2] M.S. Briggs, D.D. Burns, M.E. Cooper, S.J. Gregory, Chem. Commun. 2323-2324 (2000)
[3] M.E. Cooper, S. Gregory, E. Adie, S. Kalinka, J. Fluor. 12, 425 (2002)
[4] S.Z. Topal, F. Yuksel, A.G. Gürek, K. Ertekin, B. Yenigül, V. Ahsen, J. Photochem. Photobiol., A: Chem. 202, 205 (2009)
[5] B. Szczepanik, S. Styrcz, M. Góra, Spectrochim. Acta Part A 71, 403 (2008)
[6] D. Staneva, R. Betcheva, J-M. Chovelon, J. Photochem. Photobiol., A: Chem. 183, 159 (2006)
[7] K. Ertekin, C. Karapire, S. Alp, B. Yenigul, S. Icli, Dyes Pigm. 56, 125 (2003)
[8] S. Derinkuyu, K. Ertekin, O. Oter, S. Denizalti, E. Cetinkaya, Dyes Pigm. 76, 133 (2008)
[9] F.B.M. Suah, M. Ahmad, M.N. Taib, Sens. Act. B 90, 182 (2003)
[10] O.S. Wolfbeis, E. Furlinger, H. Kroneis, H. Marsoner, Z. Fresenius, Analyt. Chem. 314, 119 (1983)
[11] A.S. Vasylevska, A.A. Karasyov, S.M. Borisov, C. Krause, Anal. Bioanal. Chem. 387, 2131 (2007)
[12] Y. Kawabata, K. Tsuchida, T. Imasaka, N.Ishibashi, Analyt. Sci. 3, 7 (1987)
[13] D.M. Jordan, D.R. Walt, Analyt. Chem. 59, 437 (1987)
[14] M.R. Mazieres. C. Duprat, J.G. Wolf, A.D. Roshal. Dyes Pigm. 80, 355-360 (2009)
[15] M. Adamczyk, J. Grote, Bioorg. Med. Chem. Lett. 13, 2327 (2003)
[16] O.V. Grygorovych, S.M. Moskalenko, B.A. Marekha, A.O. Doroshenko, J. Fluor. 20, 115 (2010)
[17] M. Dekhtyar, W. Rettig, J. Photochem. Photobiol., A: Chem. 125, 57 (1999)
[18] Y. Xiao, M. Fu, X. Qian, J. Cui, Tet. Lett. 46, 6289 (2005)
[19] Y. Shiraishi, Y. Tokitoh, G. Nishimura, T. Hirai, Org. Lett. 7, 2611 (2005)
[20] B.M. Krasovitskii, B.M. Bolotin, Organic Luminescent Materials (VCH GmbH, Weinheim, Germany, 1988)
[21] F.R. Prieto, M. Mosquera, M. Novo, J. Phys. Chem. 94, 8536 (1990)
[22] M. Novo, M. Mosquera, F.R. Prieto, J. Chem. Soc., Faraday Trans. 89, 885 (1993)
[23] Z. Diwu, C.S. Chen, C. Zhang, D.H. Klaubert, R.P. Haugland, Chem. Biol. 6, 411 (1999)
[24] D. Piorun, A.B.J. Parusel, K. Rechthaler, K. Rotkiewicz, G. Köhler, J. Photochem. Photobiol., A: Chem. 129, 33 (1999)
[25] V. Baliah, R. Jeyaraman, Indian J. Chem. B15, 797 (1977)
[26] K. Ganapathy, R. Jeyaraman, Indian J. Chem. B17, 389 (1979)
[27] R. Jeyaraman, S. Avila, Chem. Rev.81, 149 (1981)
[28] D.M. Kneeland, K. Ariga, V.M. Lynch, C.-Y. Huang, E.V. Anslyn, J. Amer. Chem. Soc. 115, 10042 (1993)
[29] D. Grabka, W. Boszczyk, Y. Stepanenko, S. Styrcz, M. Kubik, K. Rotkiewicz, A. Danel, J. Photochem. Photobiol., A: Chem. 180, 80 (2006)
[30] L.A. Cabell, D. Perreault, E.V. Anslyn. Bioorg. Med. Chem. 5, 1209 (1997)
[31] V.G. Pivovarenko, A.V. Grygorovych, V.F. Valuk, A.O. Doroshenko. J. Fluor. 13, 479 (2003)
[32] V.F. Valuk, O.V. Grygorovych, A.O. Doroshenko, V.G. Pivovarenko. Ukr. Bioorg. Acta. 1, 79-89 (2004) (in Ukrainian) http://www.bioorganica.org.ua/UBAdenovo/pubs_11-204/Valuk_UBA_11-204.pdf)
[33] V.F. Valuk, V.G. Pivovarenko, A.V. Grigorovich, A.O. Doroshenko, Theoretical and Experimental Chemistry 40, 266 (2004) (DOI: 10.1023/B:THEC.0000041813.53353.94)
[34] A.J. Gordon, R.A. Ford, The chemist's companion. A handbook of practical data, tehniques and references (Wiley-Interscience, New York-London-Sydney-Toronto, 1972)
[35] A. Weissberger, Organic solvents. Physical properties and methods of purification (Inter-science publishers, Inc., New York, 1955)
[36] J.R. Lakowicz, Principles of Fluorescence Spectroscopy. 3rd edition (Springer Science + Business Media, LLC, Singapore, 2006)
[37] W.A. Melhuish, J. Phys. Chem. 65, 229 (1961)
[38] V.V. Aleksandrov, Acidity of Nonaqueous Solutions (Vyshcha Shkola, Kharkov, 1981) (in Russian)
[39] Z.L. Ernst, J. Menashi, Trans. Farad. Soc. Part 1, 59, 230 (1963)
[40] D. M. Himmelblau, Applied Nonlinear Programming (McGraw-Hill Book Company, New York, 1972)
[41] D.B. Siano, D.E. Metzler, J. Chem. Phys. 51, 1856 (1969)
[42] J.J.P. Stewart, J. Mol. Model. 13, 1173 (2007)
[43] J.J.P. Stewart, MOPAC2009, Stewart Computational Chemistry, (Colorado Springs, CO,

UK, 2009) http://OpenMOPAC.net.
[44] O.V. Grygorovych, A.O. Doroshenko, S.M. Moskalenko, O.V. Nevskii, V.G. Pyvovarenko, Kharkov University Bulletin, 870. Chemical Series. 17(40), 125 (2009) (in Russian) http://www-chemistry.univer.kharkov.ua/files/01_Grigorovich.pdf
[45] A.O. Doroshenko et al., Molec. Engin. 3, 353 (1994)
A.O. Doroshenko, A.V. Kirichenko, V.G. Mitina,
[46] O.A. Ponomarev, J. Photochem. Photobiol., A: Chem. 94, 15 (1996)
[47] A.O. Doroshenko, A.V. Kyrychenko, V.N. Baumer, A.A. Verezubova, L.M. Ptyagina, J. Molec. Struct. 524, 289 (2000)
[48] A.O. Doroshenko, A.V. Kyrychenko, J. Waluk, J. Fluor. 10, 41-48 (2000)
[49] D. Augustin-Nowacka, M. Makowski, L. Chmurzynski, Anal. Chim. Acta 418, 233 (2000)
[50] A. Bailistreri, L. Gregoli, G. Musumarra, A. Spalletti, Tetrahedr. 54, 9721 (1998)
[51] O.V. Grygorovych, A.O. Doroshenko, V.G. Pivovarenko, V.F. Valuk, 8th Conference on Methods and Applications of Fluorescence: Spectroscopy, Imaging and Probes (MAF8), 24-27 Aug 2003, Prague, Czech Republic, 134
[52] L.P. Hammet, Physical Organic Chemistry. Reaction rates, equilibria and mechanisms (McGraw-Hill Book Company, New York, 1970)
[53] G. Kortum, W. Vogel, R. Andrussow, Dissociation constants of organic acids in aqueous solution (Plenum Press, New York, 1961)
[54] E.M. Arnett, Prog. Phys. Org. Chem. 1, 223 (1963)
[55] C.S. Sharov, V.M. Ivanov, Moscow University Chemistry Bulletin 44, 397 (2003) (in Russian) http://www.chem.msu.ru/eng/journals/vmgu/036/abs006.html
[56] A.I. Kiprianov, Russ. Chem. Rev. 40, 594 (1971)